Electronic Supplementary Material (ESI) for Physical Chemistry Chemical Physics.
This journal is © the Owner Societies 2022

Supporting information for

"Structural, electronic phase transitions and thermal spin transport properties in 2D $NbSe_2$ and NbS_2: A first-principles study"

Yuqi Liu,[a] Yulin Feng,[b] Lei Hu,[a] Xuming Wu,[c] Shuang Qiao[d] and Guoying Gao*[a]

[a]School of Physics and Wuhan National High Magnetic Field Center, Huazhong University of Science and Technology, Wuhan 430074, China

[b]College of Physics and Electronic Science, Hubei Normal University, Huangshi 435002, China

[c]College of Physical Science and Technology, Lingnan Normal University, Zhanjiang 524048, China

[d]Beijing Computational Science Research Center, Beijing 100093, China

E-mail: guoying_gao@mail.hust.edu.cn

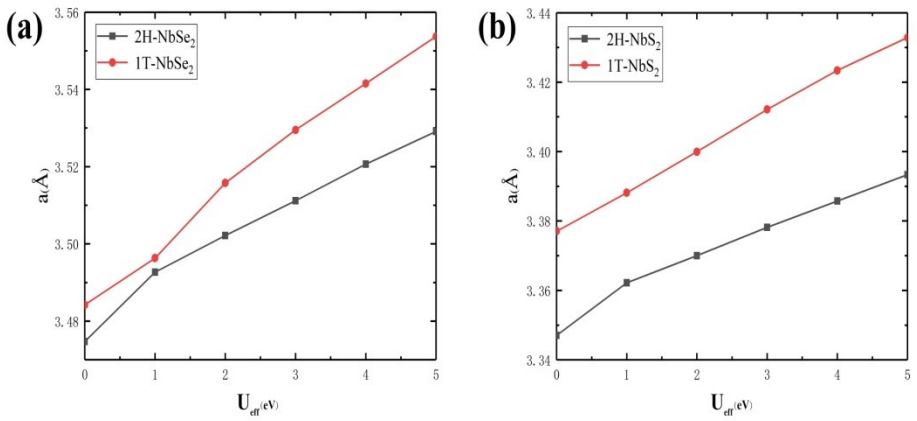

Fig. S1 The optimized lattice constants for 2H- and 1T-$NbSe_2$ (a) and NbS_2 (b) monolayers within PBE with different U values.

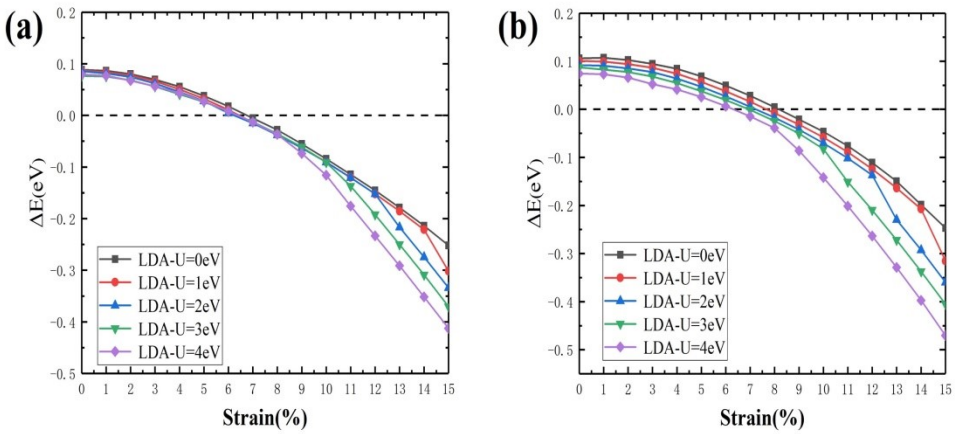

Fig. S2 The structural phase transition diagrams of (a) $NbSe_2$ and NbS_2 (b) within LDA with different U values. The total energy difference per formula unit $\Delta E = E_{1T}-E_{2H}$.

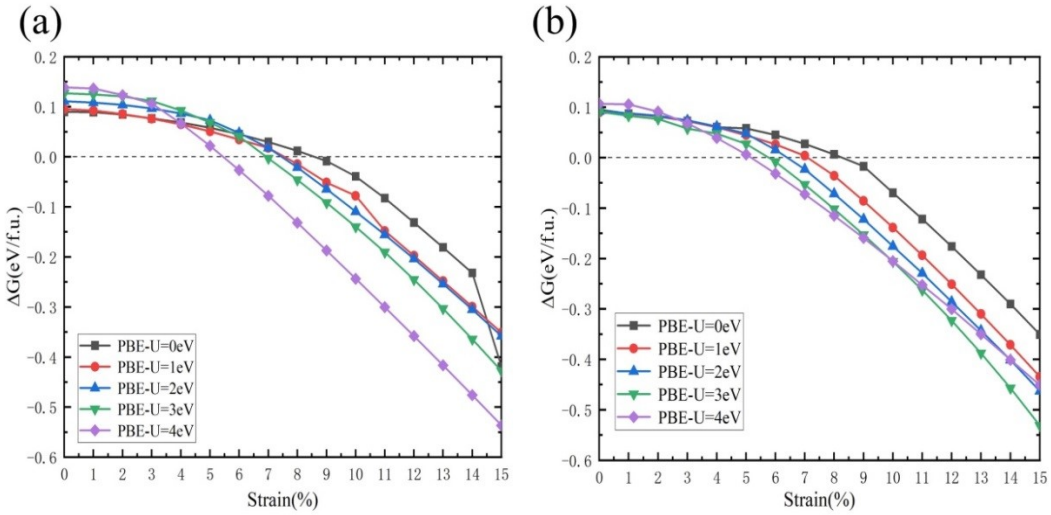

Fig. S3 The structural phase transition diagrams of (a) $NbSe_2$ and NbS_2 (b) within PBE with different U values. The Gibbs free energy difference per formula unit $\Delta G = G_{1T}-G_{2H}$.

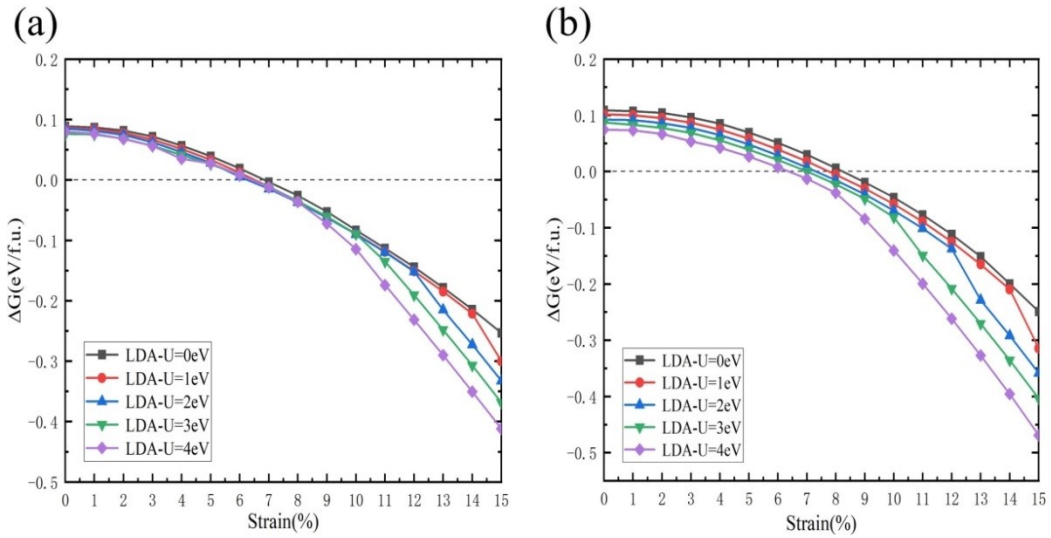

Fig. S4 The structural phase transition diagrams of (a) $NbSe_2$ and NbS_2 (b) within LDA with different U values. The Gibbs free energy difference per formula unit $\Delta G = G_{1T}-G_{2H}$.

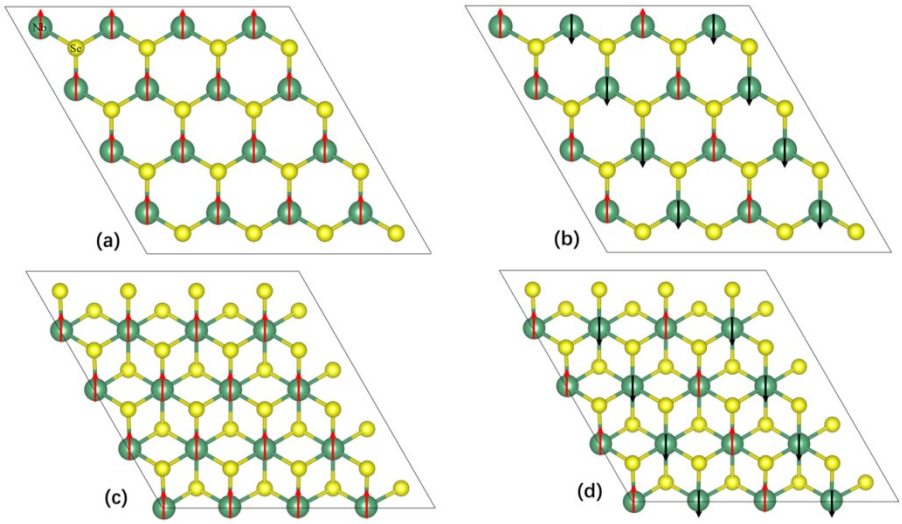

Fig. S5 The spin structures of 2H-NbX_2 (X=Se, S) with FM (a) and AFM (b) states and 1T-NbX_2 with FM (c) and AFM (d) states.

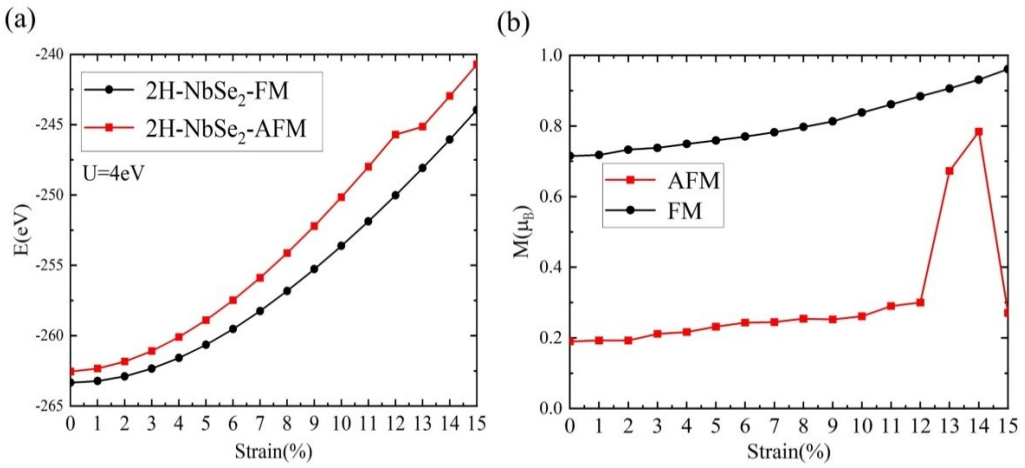

Fig. S6 The strain-dependent total energy per formula unit (a) and Nb atomic magnetic moment (b) in the FM and AFM states within PBE+U (U_{eff}=4.0 eV) for $NbSe_2$ monolayer.

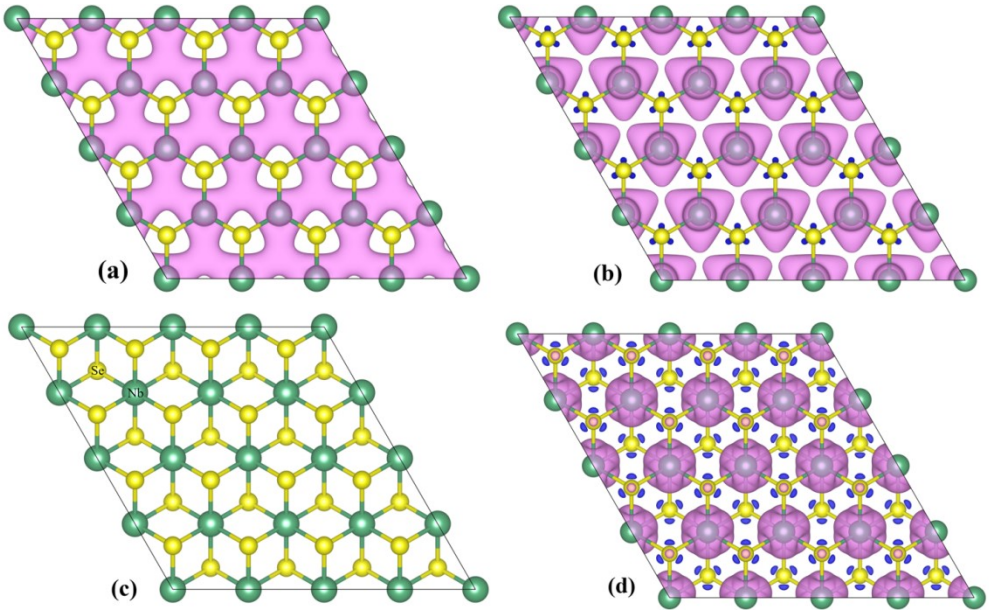

Fig. S7 The spin density within PBE+U (U_{eff}=4.0 eV) for $NbSe_2$ monolayer in the 2H (a,b) and 1T (c,d) phases. (a, c) and (b,d) represent without and with 15% tensile strain, respectively. The pink and blue isosurfaces represent the positive and negative spin densities (0.012 e/Å^2) respectively.

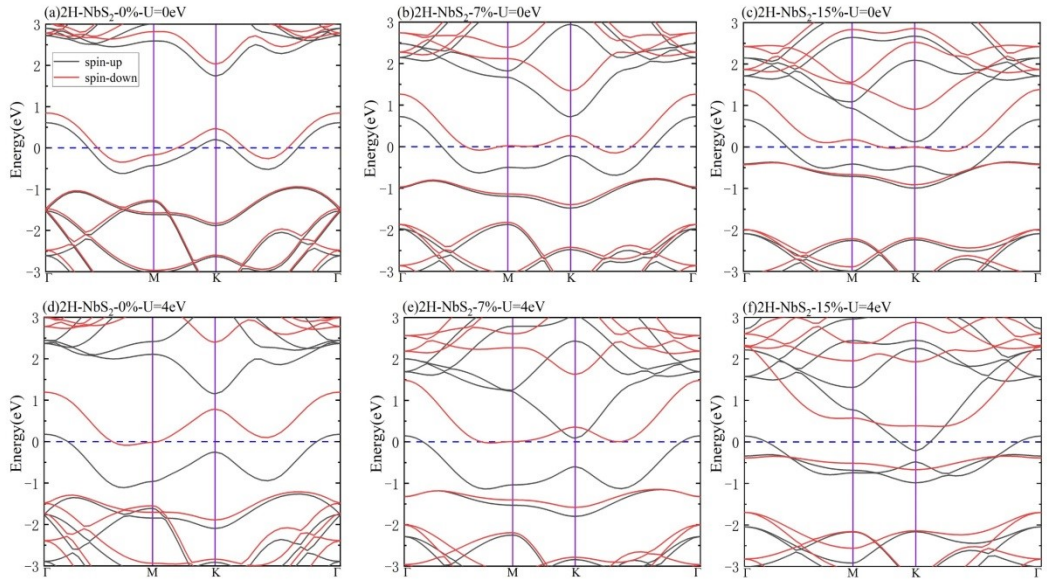

Fig. S8 Tensile strain effect on spin-polarized band structures for 2H-NbS_2 monolayer within PBE+U. The Fermi level is indicated by the blue dashed line.

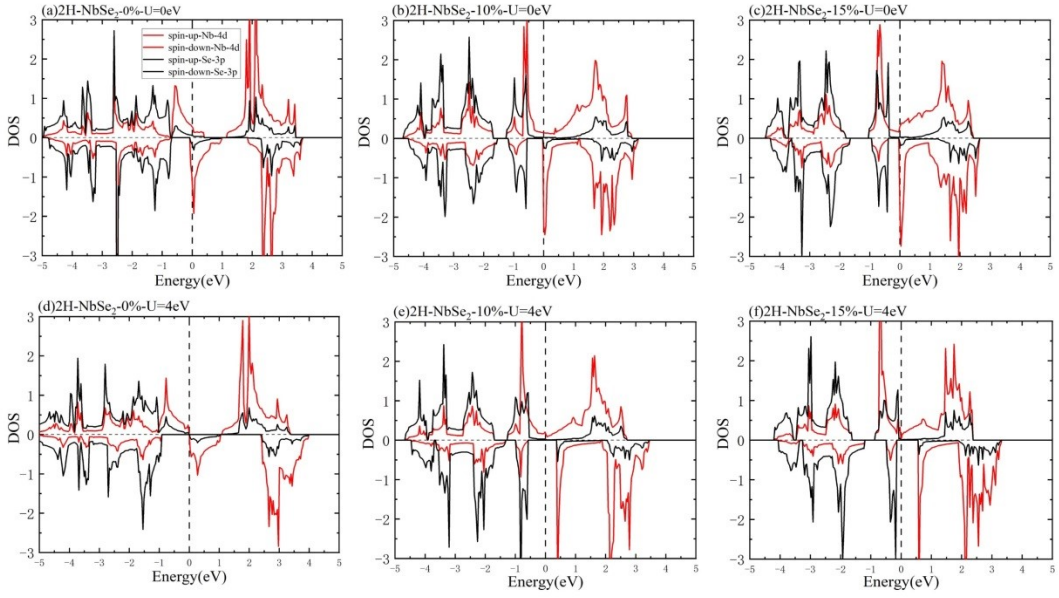

Fig. S9 Spin-dependent partial density of states (DOS) within PBE and PBE+U (U_{eff}=4.0 eV) for 2H-$NbSe_2$ monolayer with tensile strain.

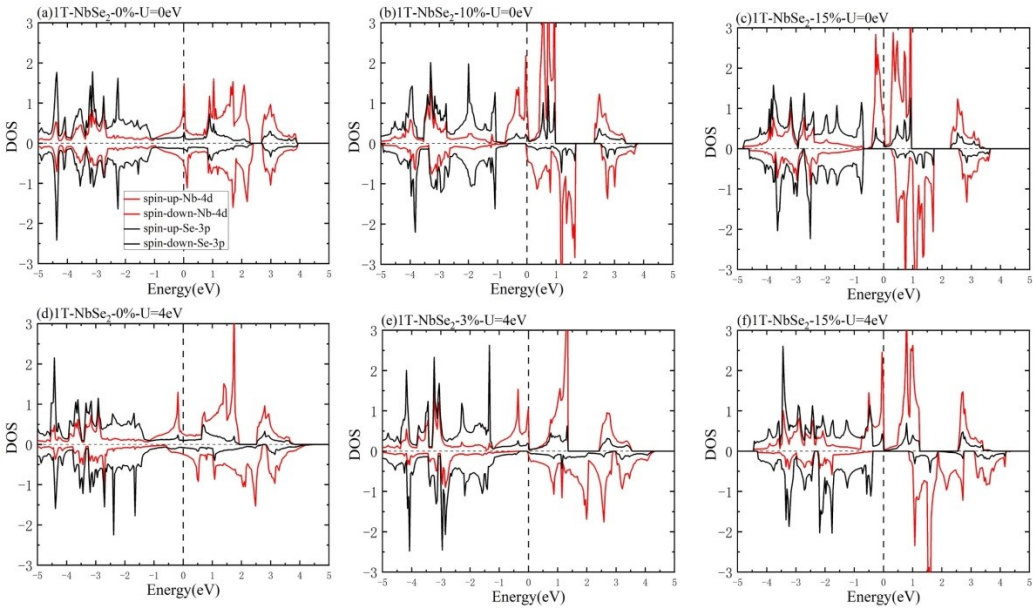

Fig. S10 Spin-dependent partial density of states (DOS) within PBE and PBE+U (U_{eff}=4.0 eV) for 1T-$NbSe_2$ monolayer with tensile strain.

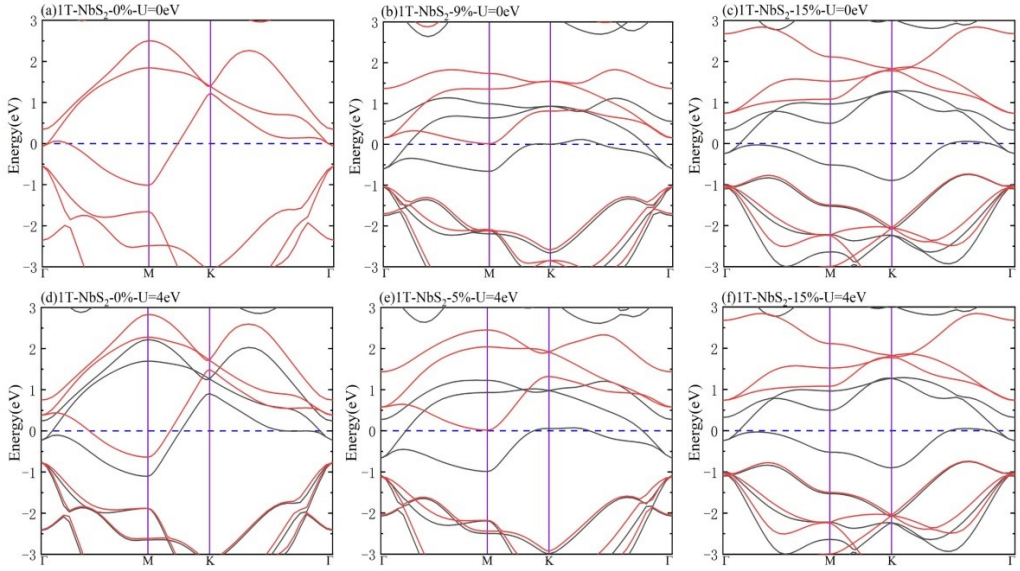

Fig. S11 Tensile strain effect on spin-polarized band structures for 1T-NbS_2 monolayer with PBE+U (U_{eff}=0, 4 eV).

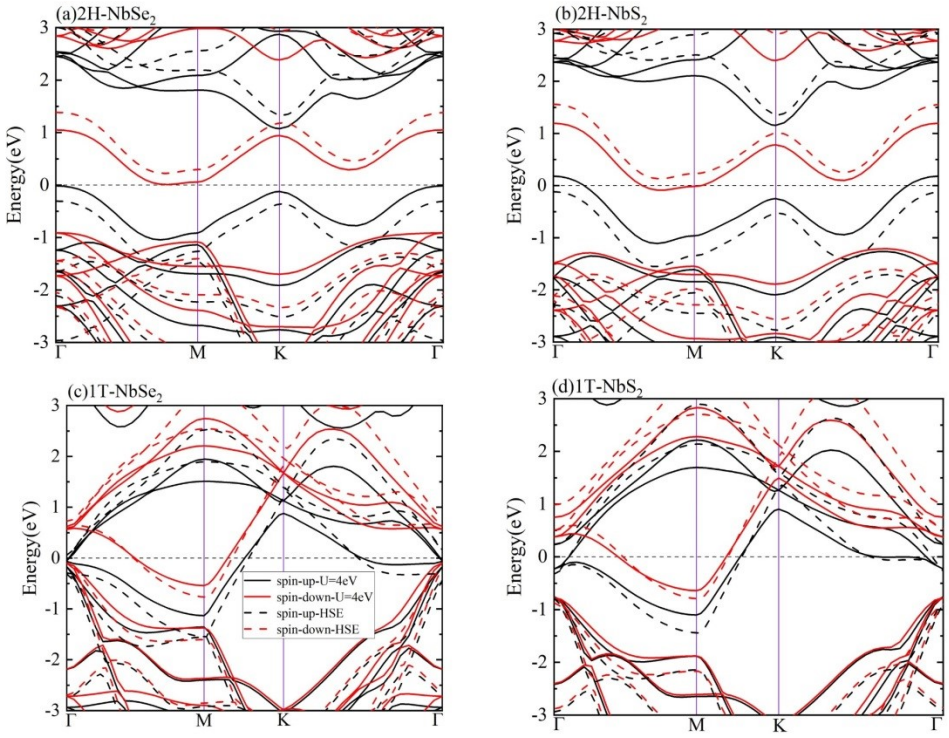

Fig. S12 Spin-polarized band structures with hybrid Heyd-Scuseria-Ernzerhof functional and PBE+U (U_{eff}= 4.0 eV) for $NbSe_2$ and NbS_2 monolayers in 2H and 1T phases.

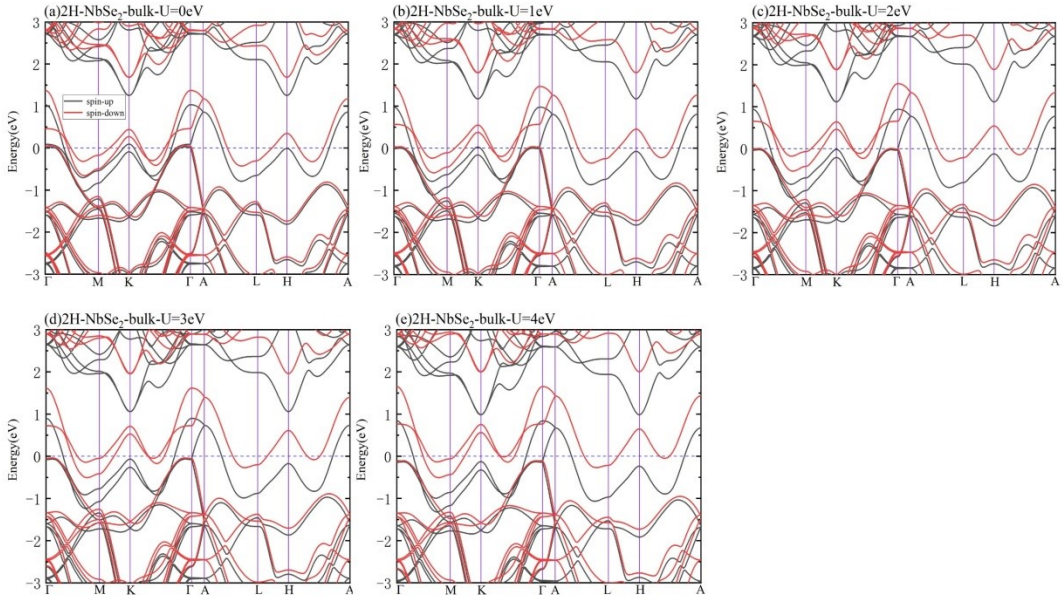

Fig. S13 Spin-polarized band structures for 2H-$NbSe_2$ bulk within PBE+U (U=0, 1, 2, 3, 4 eV).

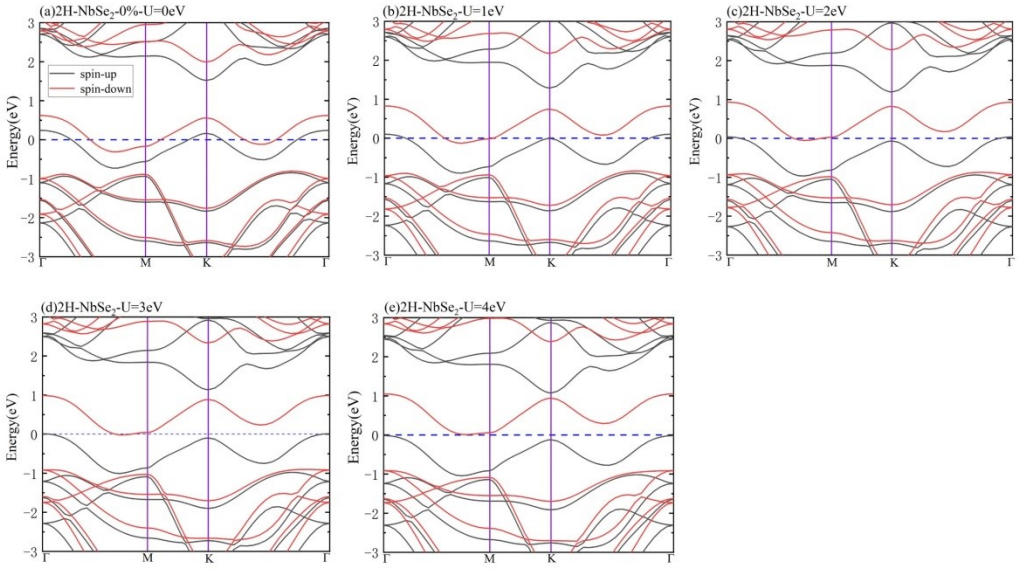

Fig. S14 Spin-polarized band structures for 2H-$NbSe_2$ monolayer within PBE+U (U=0, 1, 2, 3, 4 eV).

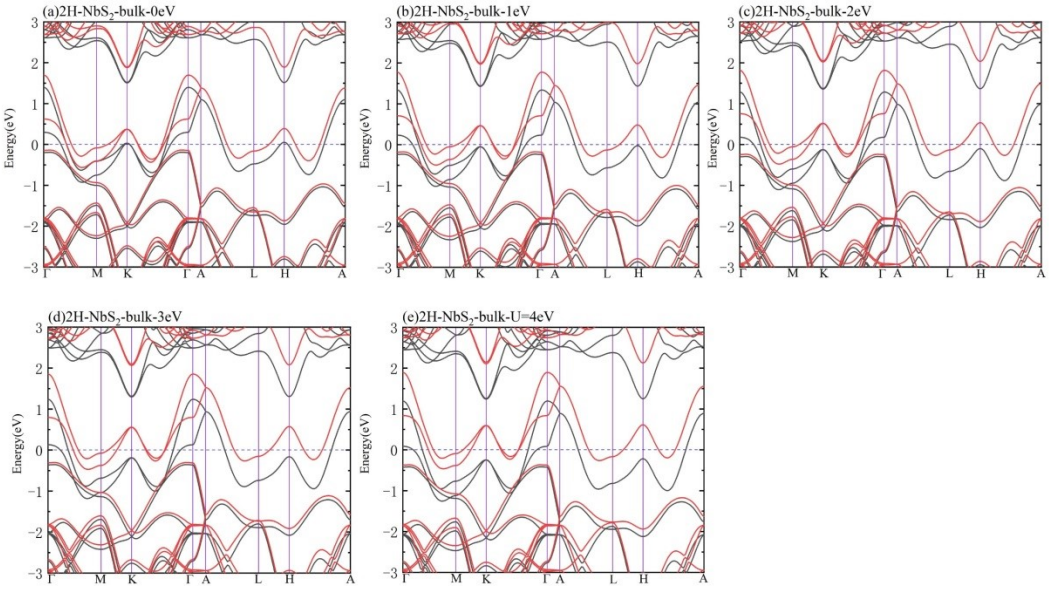

Fig. S15 Spin-polarized band structures for 2H-NbS_2 bulk within PBE+U (U=0, 1, 2, 3, 4 eV).

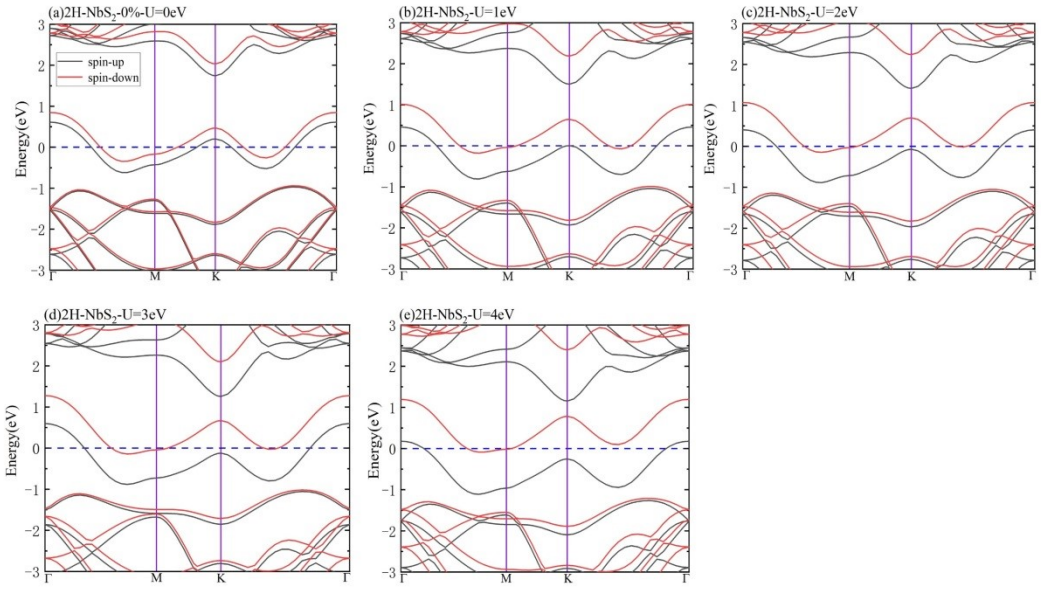

Fig. S16 Spin-polarized band structures for 2H-NbS_2 monolayer within PBE+U (U=0, 1, 2, 3, 4 eV).